INTERNATIONAL JOURNAL OF AUTOMOTIVE SCIENCE AND TECHNOLOGY

2024, VOL. 8, NO:1, 132-141 www.ijastech.org e-ISSN: 2587-0963

Examination of Mechanical Tests of CFRP Composite Material with Different Orientation Angles Used in the Automotive Industry

Ercan Şimşir[1*] and Hüseyin Bayrakçeken[1]

[1.]*Department of Automotive Engineering, Faculty of Technology, Afyon Kocatepe University, Afyon, 03200, Turkey*

Abstract

Carbon fiber-reinforced polymer (CFRP) composites with excellent mechanical properties are now widely used in various industries. Carbon fabric/epoxy composites are employed in the production of various components across professional sectors such as aerospace, construction, textiles, and automotive. In the automotive sector, the use of CFRP composite lightweight materials for emission reduction, improving crashworthiness, and enhancing fuel economy has been steadily increasing. To evaluate materials in these industries, understanding their mechanical properties, such as tensile strength and three-point bending, is crucial. In this study, four different types of carbon fiber-reinforced polymer (CFRP) materials, namely [0°/0°], [0°/90°], [±45°], and [0°/90°/+45°/-45°/-45°/-45°/+45°/90°/0°], were used to determine the optimum orientation angle and strength. The specimens with four different orientation angles underwent tensile and three-point bending tests. Three-point bending tests were conducted according to ASTM D7264 standards, and tensile tests were performed in accordance with ASTM D3039 standards. It was observed that the mate-rial type that withstood the maximum force the most was the C_4^8 CFRP material with an 8-layer [0°/90°/+45°/-45°] arrangement. The maximum stress values in the three-point bending test were 258.2, 275.0, 70.1, and 285.2 Newtons for C_1^8, C_2^8, C_3^8, and C_4^8 materials, respectively. The stress value of the C_4^8 specimen increased by 10.44%, 4.74%, and 307.23% compared to C_1^8, C_2^8, and C_3^8 materials, respectively. Additionally, the % elongation in the tensile test decreased by 286.36%, 46.55%, and 73.96%, respectively. However, it was concluded that the bearing capacity of the C_4^8 specimen was higher than that of the specimens with different fabric orientations.

Keyword: Three-point bending behavior, Tensile test, CFRP composite, Automotive weight re-duction

Research Article

History
Received 04.12.2023
Revised 19.01.2024
Accepted 25.01.2024

Contact
* Corresponding author
Ercan ŞİMŞİR
esimsir@aku.edu.tr
Address: Automotive Engi neering Department, Faculty of Technology, Afyon Kocatepe University, Afyon, Turkey
Tel: +902722182547

***To cite this paper*:** Şimşir, E., Bayrakçeken, H. Examination of Mechanical Tests of CFRP Composite Material with Different Orientation Angles Used in the Automotive Industry. International Journal of Automotive Science and Technology. 2024; 8 (1): 132-141. http://dx.doi.org/10.29228/ijastech..1399886

1. Introduction

Recently, with the increased use of plastics in vehicles, the importance of plastics in the automotive industry has grown. Moreover, the utilization of various types of composite materials has risen in the automotive sector, as well as in many other areas. Composite materials are structural materials formed by combining at least two or more components without dissolving into each other [1,2]. Composites consist of a matrix formed by combining a bulk material with fiber reinforcement. While the fibers bear most of the tensile and compressive loads, the matrix transfers the load between the fibers and prevents direct contact of the fibers with the environment [3].

Fiber-reinforced polymer composites, comprising fibrous parts consisting of fibers in a polymer matrix, are utilized in the production of numerous lightweight products. Their strength and performance depend on the strength of the fibers, the chemical structure of the matrix, and the surface of the fiber matrix interface [4-6]. Fiber angles directly influence the mechanical properties of composites [3,6]. In general, composite fibers can be produced in bundles, woven fabrics, and mat forms to meet specific requirements [6,7].

Carbon fiber reinforced polymers (CFRPs) are popular lightweight materials widely used in aerospace, shipbuilding, wind turbines, the automotive industry, and various other fields. They are known for their high stiffness, strength, fatigue resistance, and corrosion resistance [8-14]. Additionally, CFRP applications are expanding into high value, lightweight consumer products, including medical devices, sports equipment, construction, and civil industries [15-17]. It is crucial to maintain the mechanical properties of lightweight materials even under varying environmental conditions [18,19]. Recently, growing concerns about environmental

pollution, fuel consumption, and crash safety have heightened efforts toward achieving safer and lighter energy absorption [20,21].

There is a growing trend towards the use of lightweight materials to achieve emission reduction, enhance crashworthiness, and improve fuel economy in automotive applications [22-25]. Many automotive industries are planning to manufacture core vehicle parts, including CFRP body panels and chassis, using carbon fiber-epoxy composite materials and other composites [26,27]. These composite materials serve as energy absorbers in vehicles, contributing to increased crashworthiness and reduced weight in key components [28-30]. Scientists worldwide have extensively investigated the crashworthiness of composite materials due to the possibility of multiple crashes during vehicle use. Examples include the bumper beam, a passive safety system, and various energy absorbing structures [31-36]. As a result, CFRPs are gaining increasing importance, gradually replacing traditional materials and leading to higher production rates [37].

When similar studies are examined in the literature, Baba M.N [38] compared two different orientations, [0/-45/45/45/90]s and [90/45/-45/0]s, using CFRP composites and concluded that the [0/-45/45/45/90]s material is more durable than the [90/45/-45/0]s material. Muhammed Y.S. and Abdelbary A. conducted tensile tests on CFRP composites with 0°, 30°, 45°, 60°, and 90° fiber orientations, finding that the maximum tensile stress occurred at a 45° fiber orientation [39]. Patel H. and Dave H. employed three fiber orientations of CFRP, [0°/90°], [30°/60°], and [45°/-45°]. The highest tensile strength was obtained at the 0°/90° orientation as a result of tensile tests [40]. Banakar P. and Shivananda H.K. investigated the mechanical properties of CFRP with ±30°, ±45°, and ±90° fiber orientations. In their research, the tensile test showed high strength properties at the 90° fiber orientation due to the even distribution of the applied tensile force to the fibers [41]. However, Keshavamurthy et al. observed that the maximum yield strength, stiffness, and load carrying capacity of GFRE composites occurred at the 0° fiber orientation [42]. Bassey et al. presented an experimental and analytical study on the effect of fiber orientation on the tensile strength of GFRP composites using the Taguchi experimental technique. They suggested that a 45° fiber orientation and 50% fiber content resulted in optimum tensile strength for the tested composite [43].

In connection with the studies mentioned above, it has been emphasized that fiber orientation plays a crucial role in determining the mechanical properties of GFRP composites. However, there is no clear consensus on the optimal orientation. Therefore, further research is needed to enhance the existing literature. In this study, carbon fiber/epoxy composite structures with four different orientation angles, namely [0°/0°], [0°/90°], [±45°] and [0°/90°/+45°/-45°/-45°/+45°/90°/0°], were compared. Additionally, three-point bending and tensile tests were conducted following ASTM D7264 / ASTM D 3039 [44,45] standards. It is anticipated that this study will make a valuable contribution to the existing literature.

2. Materials and Methods

In this study, mechanical properties of CFRP composite materials with different orientation angles were obtained and compared. The production method involved pressing under constant temperature using the hand lay-up method. Three-point bending and tensile test specimens were pre-pared from the CFRP composite plates according to ASTM standards. The CFRP composite plate materials were divided into four different groups. The number of layers in the composite specimens was designed as 8 layers in all four groups, with an average layer thickness of 2 mm. The orientation angles of the composite specimens are provided in Table 1. To facilitate the comparison of layer orientation angles for all specimens, C_1^8, C_2^8, C_3^8, and C_4^8 groups were formed. The properties of the CFRP composite plates to be used in the experiments are outlined in Table 1.

Table 1. Properties of CFRP composite plates.

Name	Orientation Angle
C_1^8	**[**0°/0°/0°/0°/0°/0°/0°/0°**]**
C_2^8	**[**0°/90°/0°/90°/0°/90°/0°/90°**]**
C_3^8	**[**+45°/-45°/+45°/-45°/+45°/-45°/+45°/-45°**]**
C_4^8	**[**0°/90°/+45°/-45°/-45°/+45°/90°/0°**]**

C_x^y: C: carbon fiber y: number of layers x: group number

2.1. Preparation of CFRP Composite Sample Plate

MGS L285 and MGS H285 were used as resin and hardener materials in sample production. In each of the 8 plates produced, 70 grams of resin material and 28 grams of hardener material were added with the help of a precision balance. The two were then mixed in a container using a mixer for 5 minutes. The sample piece was prepared by applying the epoxy material, prepared in 8 layers, onto the fiber fabrics with the aid of a brush. Each of the prepared sample pieces was subjected to 30 minutes under 5 tons of compression pressure in the press device heated to 80 degrees, as shown in Figure 1a. Subsequently, under the same pressure, the press temperature was increased to 120 degrees for another 60 minutes. The device was turned off, and the sample piece was removed from the press after approximately 45 minutes for gradual cooling.

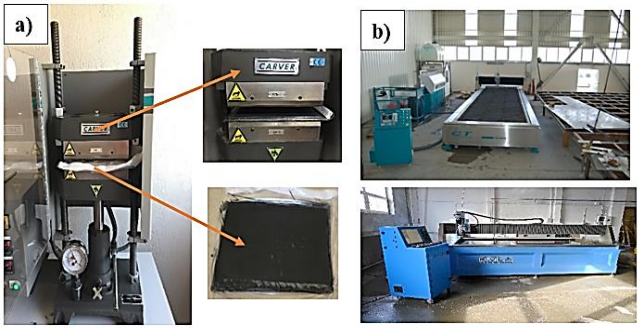

Fig. 1. a) Adjustable hot press machine b) CNC Water Jet Siemens a3216 R-HP

To obtain tensile and three-point bending specimens from the prepared specimen plates of each orientation angle, CFRP plates with different orientation angles were cut to the desired dimensions using the CNC water jet shown in Figure 1b. The Siemens a3216 R-HP series technology was employed, allowing the cutting of almost all artificial and natural materials ranging from 0.1 mm to 200 mm in thick-ness. The maximum positioning speed is 30,000 mm/min, the maximum accurate cutting speed is 10,000 mm/min, the pump flow rate is 5.5 l/min, the power is 90 kW (125 HP), and the pressure is 6000 bar.

2.2. CFRP Plate Production with Different Orientation Angles

In the production phase, a total of 8 rectangular CFRP plates, 2 for each orientation angle (C_1^8, C_2^8, C_3^8 and C_4^8), with dimensions of 250 x 180 mm, as shown in Figure 2, were produced using 300 grams/m^2 CFRP.

Fig. 2 CFRP composite plate with different orientation angles of C_1^8, C_2^8, C_3^8 and C_4^8

From the first plate of each orientation angle of CFRP composite material produced, 7 tensile specimens with dimensions of 25 x 250 mm, as shown in Figure 3, were obtained by cutting with the help of a CNC Water Jet machine. From the second plate, 10 three-point bending specimens of 10 x 100 mm were cut and obtained.

Fig. 3. CFRP composite tensile and three-point bending test specimen with different orientation angles of C_1^8, C_2^8, C_3^8 and C_4^8

2.3. Three-Point Bending Test

For the three-point bending test conducted in the study, a total of 12 specimens were tested, with 3 specimens for each orientation angle (C_1^8, C_2^8, C_3^8 and C_4^8). The test specimens were 100 mm in length, 10 mm in width, and 2 mm in wall thickness. Three-point bending tests were carried out using a Shimadzu Autograph tensile machine with a capacity of 10 kN at Afyon Kocatepe University Metallurgical and Materials Engineering Composites Laboratory. The tests were performed in accordance with ASTM D7264 standard [46]. Figure 4 illustrates the three-point bending test setup for the carbon fiber material used in the study and the testing device. The distance at the bottom of the carbon fiber material was set at 60 mm between the bearings. The ratio between the bearings was kept greater than 10, and the feed rate of the upper jaw was entered into the computer program as 10 mm/min.

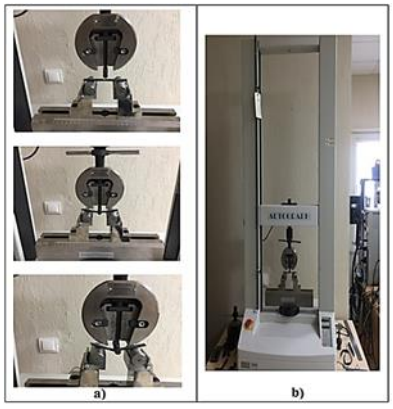

Fig. 4. a) Three-point bending test of the prepared test samples b) AUTOGRAPH device.

In the study, parameters such as the elastic modulus (E) and flexural strength (σ max) used to characterize the integrity of the carbon fiber material were calculated. The displacement and load graphs of each specimen were obtained using the computer software of the test machine. The static bending strength of the carbon fiber material is determined by the following equation for the maximum bending strength values obtained through the three-point bending test [46].

$$\sigma f = 3FL / 2bh2 \quad (1)$$

In the equation, b is the width of the specimen, σf is the bending stress, h is the thickness of the specimen, F is the maximum applied force and L is the distance between the supports.

2.4. Tensile Test

A tensile test is a procedure in which a specimen is subjected to a tensile force in one axis until it breaks, used to determine the behavior of the specimen. Tensile tests on the prepared specimens were conducted in accordance with ASTM D 3039 standards [45]. All tensile tests were performed at a speed of 5 mm/minute and at an ambient temperature of 23 ± 1°C. In the tensile test, the specimen is placed in the machine, and a tensile force is applied until it

breaks. The amount of elongation in the standard section during the application of force is recorded reciprocally to the applied force. The data on the amount of elongation were calculated using Equation 2 below.

$$\varepsilon = \frac{\Delta L}{L_0} = \frac{L - L_0}{L_0} \quad (2)$$

ΔL is the strain in length, L0 is the initial length and L is the final length. In Equation 3, the stress was calculated using the force data.

$$\sigma = \frac{F_n}{A} \quad (3)$$

σ is stress, F is force, and A is standard cross-sectional area.

2.4.1. Preparation of silicone mold for the jaw part of the tensile test specimen

To ensure accurate results during the tensile test, a silicone mold was prepared for the tensile specimens, as shown in Figure 5, to protect the end part of the carbon fiber material from damage by the jaws of the testing device. The iron mold parts were cut using a CNC laser machine.

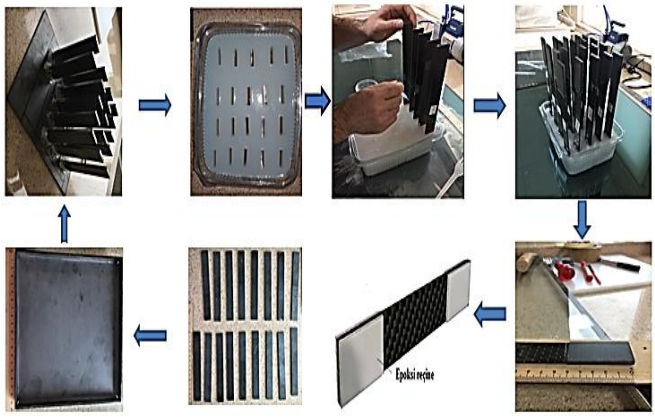

Fig. 5. Production stages of the silicone mold for the jaw part of the sample and the stage of coating the jaw parts of the tensile test sample with epoxy

After preparing the silicone mold, the jaw parts of the tensile specimens were inserted into the mold, as shown in Figure 5, and the prepared epoxy mixture was poured into the intermediate gaps. With the mold, the jaw parts of 20 tensile specimens were cured with epoxy material simultaneously. The curing time was approximately 24 hours. Subsequently, the specimens were turned, and the other end jaw parts were placed in the mold and cured with epoxy. After completing these process steps, the carbon fiber test specimen was ready for the tensile test.

2.4.2. Universal Tensile Testing Machine

Tensile tests on carbon fiber materials with different orientation angles were conducted using the Shimadzu AG-X universal tensile testing machine at the Composites Research Laboratory in the Department of Mechanical Engineering, Dokuz Eylül University, Izmir. Figure 6a displays an image of the tensile testing machine and the connection of the specimen to the testing machine.

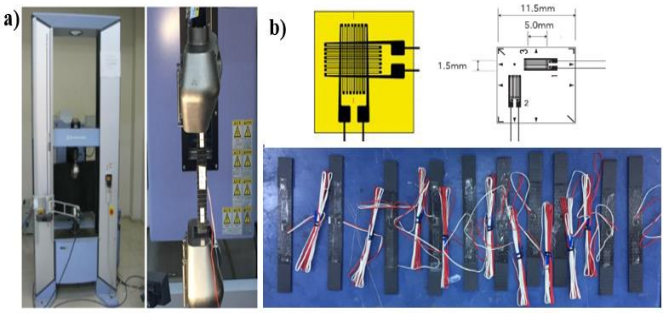

Fig. 6. a) Shimadzu AG – X tensile device b) Bonding of strain gauges to the tensile test sample.

A total of 10 tensile test specimens, including 2 with C_1^8, 3 with C_4^8, 2 with C_2^8, and 3 with C_3^8 orientation angles, were prepared, as shown in Figure 6b. UBF series 0°/90° biaxial BFCA 2-3 strain gauges (shown in Figure 6b) were used to measure values such as elastic modulus and Poisson's ratio for each of the tensile test specimens. A Data Logger TDS-530 multi-channel scanning data logger was used to read the data from the strain gauges connected to the specimen. The data received from the Data Logger were transferred to the Shimadzu/Trapezium program interface software used in the computer environment, and the data of the tensile sample were recorded.

3. Results and Discussion

In this study, three-point bending tests were experimentally investigated for materials with C_1^8, C_2^8, C_3^8 and C_4^8 orientations. The maximum and average force values of the specimens subjected to three-point bending tests were calculated, and stress strain graphs were created based on the obtained data.

3.1. Three Point Bending Test Results with C_1^8, C_2^8, C_3^8 and C_4^8 Orientation Angle

Three test specimens were used for the three-point bending test of the produced C_1^8 orientation angle carbon fiber material. Among the three different three-point bending tests, the C_1^8-1 test specimen demonstrated the best strength, as shown in Figure 7a, with a flexural strength of 597.7 MPa. In Figure 7b, the C_2^8-3 test specimen exhibited the best strength, and its flexural strength was 654.8 MPa. Figure 7c displays the C_3^8-2 test specimen with the best strength and a flexural strength of 194.5 MPa. Figure 7d showcases the C_4^8-3 test specimen with the best strength, and its flexural strength is 739 MPa. Observing the graphs in Figure 7, it is evident that there are sudden drops and rises in the C_1^8, C_2^8, and C_4^8 orientation angles.

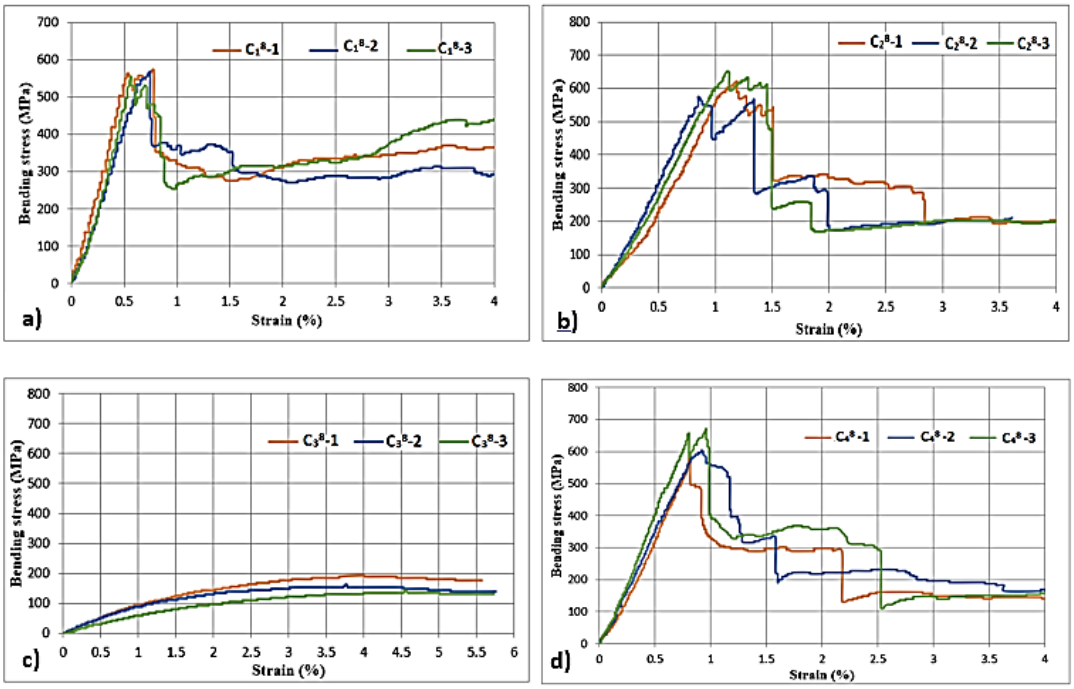

Fig. 7 Three-point bending test graphs of the sample with C_1^8, C_2^8, C_3^8 and C_4^8 orientation angles

This phenomenon is attributed to the number of layers in the specimens, indicating layer breakage.

The average values of carbon fiber specimens with C_1^8, C_2^8, C_3^8, and C_4^8 orientation angles are depicted in Figure 8. The specimen with the C_4^8 orientation angle exhibited the best result among the three-point bending specimens. The fiber orientation angle used in the C_4^8 specimen indicates that it carries more load than other orientation angles.

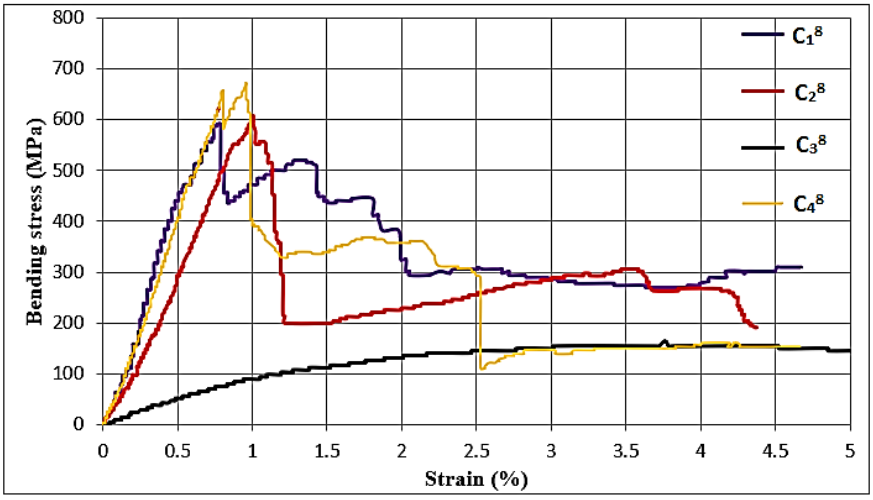

Fig. 8 Three-point bending plot of average samples C_1^8, C_2^8, C_3^8 and C_4^8

Three test specimens each were subjected to a three-point bending test for C_1^8, C_2^8, C_3^8, and C_4^8orientation angle CFRP composite materials. Table 2 presents the thickness, width, cross sectional area of the specimen, distance between supports, maximum stress, maximum force, maximum displacement, and maximum strain for C_1^8, C_2^8, C_3^8, and C_4^8specimens, respectively. The stress value of the C_4^8 composite material in the three-point bending test is higher than that of the other orientation angle composite materials. After the three-point bending test, the maximum force values are 258.2 N, 275.0 N, 70.1 N, and 285.2 N for C_1^8, C_2^8, C_3^8, and C_4^8 materials, respectively. It was observed that the C_4^8 composite material increased by 10.44% compared to C_1^8 material, 4.74% compared to C_2^8 material, and 307.23% compared to C_3^8 material.

Table 2. Bending test results of the sample with C_1^8, C_2^8, C_3^8 and C_4^8orientation angles

Orientation angle	Sample No	Max. Stress (MPa)	Max. Force (N)	Max. Substitution (mm)	Max. Elongation (%)
C_1^8	No. 1	585,9	260,4	2.20	0,734
	No. 2	574,6	255,3	1.97	0,658
	No. 3	566,4	251,7	1.76	0,5883
	Average	**581,1**	**258,2**	**2.07**	**0,6917**
C_2^8	No. 1	618,7	275,0	3.12	1,042
	No. 2	574,5	255,3	2.67	0,891
	No. 3	654,8	291,0	3.30	1,103
	Average	**618,7**	**275,0**	**3.12**	**1,042**
C_3^8	No. 1	194,5	86,4	12.14	4,04
	No. 2	159,3	70,8	11.32	3,77
	No. 3	140,0	62,2	13.68	4,56
	Average	**157,6**	**70,02**	**13.12**	**4,37**
C_4^8	No. 1	605,8	269,2	2.32	0,77
	No. 2	659,2	293,0	2.89	0,96
	No. 3	739,0	328,4	2.83	0,94
	Average	**641,8**	**285,2**	**2.62**	**0,87**

3.2. C18, C28, C38 and C48 Orientation Angle Tensile Test Results

A total of 8 tensile test specimens with C_1^8, C_2^8, C_3^8, and C_4^8 orientation angles were examined experimentally. Each material with different orientation angles was evaluated in the tensile test. The types of damage, such as fiber breaks and tears, that occurred in the test specimens with different orientation angles as a result of the tensile test are shown in Figure 9.

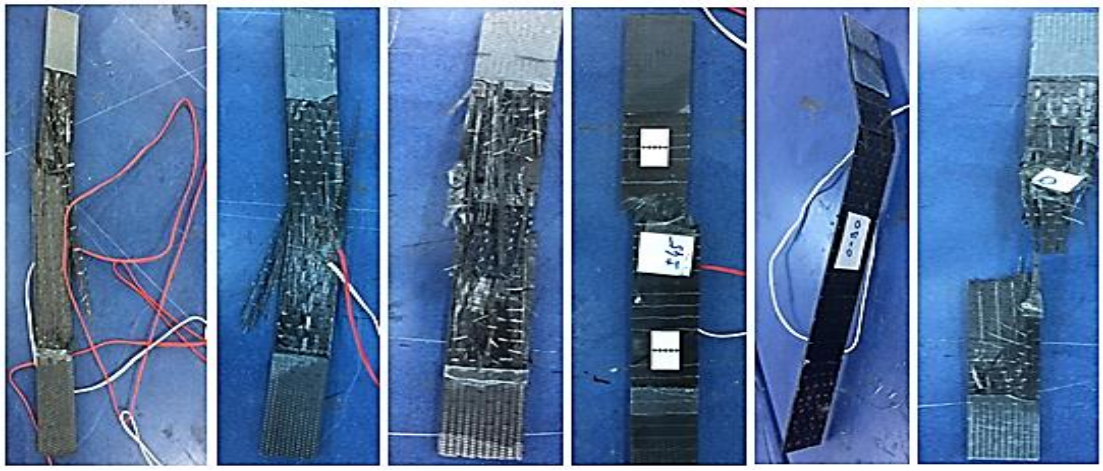

Fig. 9. Damage images on the samples as a result of the tensile test.

Maximum stress, elastic modulus, maximum displacement, and maximum forces were calculated from the data obtained from each tensile test specimen. The CFRP composite material with C_2^8 orientation exhibited the best result values, while the CFRP composite material with C_4^8 orientation had the closest results. Fiber breaks and fractures were observed in the CFRP composite materials.

The force/extension graph of 2 C_1^8 orientation angle carbon fiber materials prepared as a result of the tensile test is shown in Figure 10. In Figure 10a, the highest maximum force is 38.45 kN

in the C_1^8-1 test specimen. In Figure 10b, the highest maximum force is 43.39 kN for the C_2^8-2 test specimen. In Figure 10c, the highest maximum force is 3.85 kN in the C_3^8-2 test specimen.

In Figure 10d, the highest maximum force is 33.17 kN in the C_4^8-2 test specimen. The highest strength value of the test specimens was obtained from the C_2^8-2 test specimen. Looking at Figure 10, sudden drops indicate that the tensile specimen is completely broken.

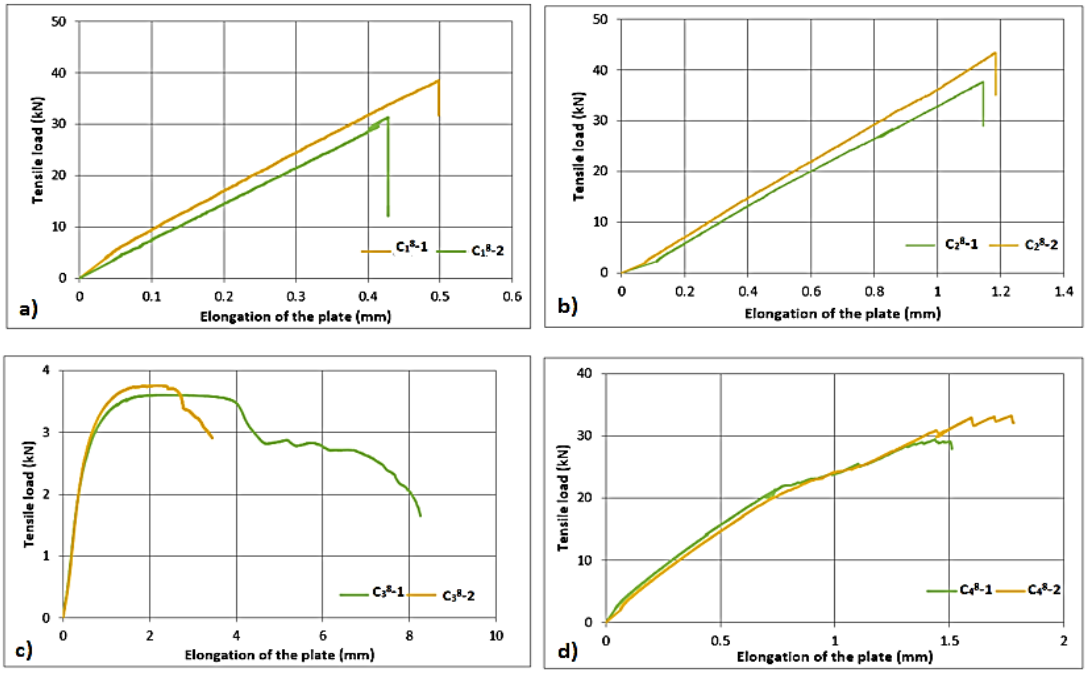

Fig. 10 Force/elongation graphs of test samples with C_1^8, C_2^8, C_3^8 and C_4^8orientation angles

The data obtained from the graphs are summarized in Table 3. Accordingly, the average maximum tensile strengths of CFRP composite materials with C_1^8, C_2^8, C_3^8, and C_4^8 orientation angles were 34.90 kN, 40.54 kN, 3.73 kN, and 31.24 kN, respectively. The average moduli of elasticity were 157.8 GPa, 75.6 GPa, 10.0 GPa, and 52.4 GPa, and the average percentage elongations were 0.44, 1.16, 6.53, and 1.7, respectively.

In the row section of the table, the thickness, width, cross-sectional area, distance to the extensometer, modulus of elasticity, maximum stress, maximum force, Poisson's ratio, and percent elongation are given, respectively. In the column section, specimen numbering is provided.

Table 3. Tensile test numerical values of the sample with C_1^8, C_2^8, C_3^8 and C_4^8 orientation angles

Orientation angle	Sample No	a0 mm	b0 mm	S0 mm²	L0 mm	E-Module GPa	Max-Stress-MPa	Max-Force kN	Poisson's Ratio	Elongation %
C_1^8	No. 1	1,9	25	47,5	102	161.1	809.6	38.45	0.3029	0.48
	No. 2					154.6	660.1	31.35	0.3581	0.41
	Average					157.8	734.8	34.90	0.3305	0.44
C_2^8	No. 1	1,9	25	47,5	100	77.6	793.7	37.70	0.4156	1.07
	No. 2					73.6	913.5	43.39	0.4605	1.25
	Average					75.6	853.6	40.54	0.4380	1.16
C_3^8	No. 1	1,9	25	47,5	103	9.5	75.8	3.60	0.5432	8.1
	No. 2					10.5	78.8	3.74	0.6190	3.3
	Average					10.0	78.5	3.73	0.5811	6.53
C_4^8	No. 1	1,9	25	47,5	103	59.2	619.2	29.41	0.2510	1.5
	No. 2					47.3	698.4	33.17	0.3367	1.7
	Average					52.4	657.7	31.24	0.2938	1.7

The average values of each of the C_1^8, C_2^8, C_3^8, and C_4^8 orientation angle carbon fiber samples were calculated. It was observed that the % elongation of the composite material with a C_4^8 orientation angle increased by 286.36% compared to the C_1^8 material, increased by 46.55% compared to the C_2^8 material, and decreased by 73.96% compared to the C_3^8 material.

4. Conclusion

In this study, three-point bending and tensile tests were experimentally conducted on C_1^8, C_2^8, C_3^8, and C_4^8 CFRP composite materials with four different orientation angles. The following results were obtained from the studies.

1-) In the epoxy matrix composite materials used in the study, it was observed that the elongation until damage varied between 0.44% in the C_1^8 group, 1.16% in the C_2^8 group, 6.53% in the C_3^8 group, and 1.7% in the C_4^8 group. Although the fibers exhibit dominant properties in the tensile direction, this difference is attributed to the movement of the fibers within the epoxy matrix.

2-) In their study, Tawfek et al. [48] asserted that the arrangement of various orientation angles in CFRP composites directly influences the material's strength. They concluded that composites with a (0/90/±45)° reinforcement angle exhibit higher strength values compared to composites with a (0/0/90/90/90)° reinforcement angle. Our study similarly found that composite materials with a C_4^8 orientation angle demonstrated superior strength compared to composites with other orientation angles, thus corroborating existing literature.

3-) In 8-layer specimens, the maximum force followed the order: $C_4^8 > C_1^8 > C_3^8 > C_2^8$. The highest contact force was observed in the C_4^8 material with the [0°/90°/+45°/-45°/-45°/-45°/+45°/90°/0°] arrangement, while the lowest contact force was recorded in the C_2^8 composite material with the [0°/90°/0°/0°/90°/0°/0°/90°/0°/90°/0°/90°] arrangement.

4-) The stress value of the C_4^8 composite material in the three-point bending test exceeds that of other orientation angle composite materials. Following the three-point bending test, the maximum forces recorded were 258.2 N for C_1^8, 275.0 N for C_2^8, 70.1 N for C_3^8, and 285.2 N for C_4^8. Notably, the C_4^8 composite material exhibited a 10.44% increase compared to C_1^8, a 4.74% increase compared to C_2^8, and a remarkable 307.23% increase compared to C_3^8.

5-) The maximum stresses in the tensile test for C_1^8, C_2^8, C_3^8, and C_4^8 materials were 734.8 MPa, 853.6 MPa, 78.5 MPa, and 657.7 MPa, respectively. Notably, C_2^8 material exhibited the highest stress value, while C_3^8 material showed the minimum stress value. The higher stress in C_2^8 material can be attributed to the alignment of fibers in the tensile direction, a finding consistent with the study conducted by Banakar P. and Shivananda H.K [41].

6-) The % elongation of the C_4^8 composite material in the tensile test increased by 286.36% compared to C_1^8, by 46.55% compared to C_2^8, and decreased by 73.96% compared to C_3^8.

7-) Among the carbon fiber composite materials with four different orientation angles examined in the test results, the C_4^8 orientation angle carbon fiber material with the sequence [0°/90°/+45°/-45°/-45°/-45°/+45°/90°/0°] yielded the best result. This outcome aligns with the findings of Muhammed Y.S. and Abdelbary A [39], as well as Bassey et al. [43].

Acknowledgment

The scattered investigations in this study were carried out with the budget provided by Afyon Kocatepe University "17 SCIENCE No. 65" Scientific Research Projects Coordination (BAPK) project.

Nomenclature

CFRP : Carbon Fiber Reinforced Polymer

C_1^8 : [0°/0°/0°/0°/0°/0°/0°/0°]

C_2^8 : [0°/90°/0°/90°/0°/90°/0°/90°]

C_3^8 : [+45°/-45°/+45°/-45°/+45°/-45°/+45°/-45°]

C_4^8 : [0°/90°/+45°/-45°/-45°/+45°/90°/0°]

Conflict of Interest Statement

The authors declare that there is no conflict of interest in the study.

CRediT Author Statement

Ercan Şimşir: test sample production and mechanical tests, Written-original,
Hüseyin Bayrakçeken: Supervision,

References

[1] Balasubramanian M. Composite materials and processing. Composite Materials and Processing 2013:1–599. https://doi.org/10.1201/B15551/Composite-Materials-Processing-Balasubramanian.

[2] Kaw AK. Introduction to Composite Materials. Mechanics of Composite Materials 2021:25–84. https://doi.org/10.1201/9781420058291-9/Introduction-Composite-Materials-Autar-Kaw.

[3] Huang S, Fu Q, Yan L, Kasal B. Characterization of interfacial properties between fibre and polymer matrix in composite ma-terials e A critical review 2021, 13: 1441-1484. https://doi.org/10.1016/j.jmrt.2021.05.076.

[4] Zhang X, Fan X, Yan C, Li H, Zhu Y, Li X, et al. Interfacial microstructure and properties of carbon fiber composites modi-fied with graphene oxide. ACS Appl Mater Interfaces 2012;4:1543–52. https://doi.org/10.1021/AM201757V.

[5] Teklal F, Djebbar A, Allaoui S, Hivet G, Joliff Y, Kacimi B. A review of analytical models to describe pull-out behavior – Fiber/matrix adhesion. Compos Struct 2018;201:791–815. https://doi.org/10.1016/J.Compstruct.2018.06.091.

[6] Katmer MC, Akkurt A, Kocakulak T. Investigation of Natural Frequency Values of Composite Cover Design with Different Laying Angles. Engineering Perspective 2022; 2;4: 46-51. http://dx.doi.org/10.29228/eng.pers.66826.

[7] Pastuszak PD, Muc A. Application of Composite Materials in Modern Constructions. Key Eng Mater 2013;542:119–29. https://doi.org/10.4028/www.Scientific.net/Kem.542.119.

[8] Singh DK, Vaidya A, Thomas V, Theodore M, Kore S, Vaidya U.

Finite Element Modeling of the Fiber Matrix Interface in Polymer Composites. Journal of Composites Science 2020;4;58. https://doi.org/10.3390/JCS4020058.
[9] Sanjay MR, Madhu P, Jawaid M, Senthamaraikannan P, Senthil S, Pradeep S. Characterization and properties of natural fiber polymer composites: A comprehensive review. J Clean Prod 2018;172:566–81. https://doi.org/10.1016/J.JCLEPRO.2017.10.101.
[10] Rani M, Choudhary P, Krishnan V, Zafar S. A review on recycling and reuse methods for carbon fiber/glass fiber composites waste from wind turbine blades. Compos B Eng 2021;215:108768.https://doi.org/10.1016/J.Compositesb.2021.108768.
[11] Supian ABM, Sapuan SM, Zuhri MYM, Zainudin ES, Ya HH. Hybrid reinforced thermoset polymer composite in energy absorption tube application: A review 2018, 14.4: 291-305. https://doi.org/10.1016/j.dt.2018.04.004.
[12] Altin Karatas M, Abant okkaya. A review on machinability of carbon fiber reinforced polymer (CFRP) and glass fiber reinforced polymer (GFRP) composite materials 2018, 14.4: 318-326. https://doi.org/10.1016/j.dt.2018.02.001.
[13] Kiersnowska A, Fabianowski W, Koda E. The Influence of the Accelerated Aging Conditions on the Properties of Polyolefin Geogrids Used for Landfill Slope Reinforcement. Polymers, 2020, 12.9: 1874. https://doi.org/10.3390/polym12091874.
[14] Bayrakçeken H, Şimşir E, Serhat Başpınar M, Atlı İS. Experimental Investigation on the Pulse Behavior of Polymeric Matrix Composites Used in Vehicles. International Journal of Science and Research 2019; 8-6: 1400-1406. 10.21275/ART20198800.
[15] Angelone R, Caggiano A, Nele L, Teti R. Optimal cutting parameters and tool geometry in drilling of CFRP/CFRP stack laminates for aeronautical applications. Procedia CIRP 2021;99:398–403. https://doi.org/10.1016/J.PROCIR.2021.03.056.
[16] Qin G, Zheng L, Mi P, Zhu Y, Li M, Na J, et al. Influence of single or multi factor coupling of temperature, humidity and load on the aging failure of adhesively bonded CFRP / aluminum alloy composite joints for automobile applications. Int J Adhes Adhes 2023;123:103345. https://doi.org/10.1016/j.ijadhadh.2023.103345.
[17] Kim W, Kim YM, Song S, Kim E, Kim D-G, Jung YC, et al. Manufacture of antibacterial carbon fiber-reinforced plastics (CFRP) using imine based epoxy vitrimer for medical application 2023. https://doi.org/10.1016/j.heliyon.2023.e16945.
[18] Hoang VT, Cho HT, Kim MJ, Hong so M, Park SH, Kweon JH, et al. Shear strength and failure modes of double-lap bi material CFRP/Ni-Cr alloy joint under severe environmental conditions. Advanced Composite Materials 2022;31:311–34. https://doi.org/10.1080/09243046.2021.2004652.
[19] Hyeon-Seok C, Byeong-Su K, Seong-Min P, Viet-Hoai T, Young-Woo N, Jin-Hwe K. Tensile strength of composite bonded scarf joint in various thermal environmental conditions. Advanced Composite Materials 2020;29:285–300. https://doi.org/10.1080/09243046.2019.1710679.
[20] Fang F, Chen N, Cai P, Zhou T, Thompson B. Perceptual learning modifies the functional specializations of visual cortical areas. J Vis 2016;16:1091–1091. https://doi.org/10.1167/16.12.1091.
[21] Şimşir E, Yavuz İ, Çağdaş ERİK M,. Taşit Tamponlarinda Kullanilan Polimer Malzemelerin Farkli Hizlarda Absorbe Edilen Enerjilerinin Karşilaştirilmasi. Konya Journal of Engineering Sciences 2021;9:932–42. https://doi.org/10.36306/KONJES.932489.
[22] Sun G, Yu H, Wang Z, Xiao Z, Li Q. Energy absorption mechanics and design optimization of CFRP/aluminium hybrid structures for transverse loading. Int J Mech Sci 2019;150:767–83. https://doi.org/10.1016/j.ijmecsci.2018.10.043.
[23] Sun G, Wei Y, Huo X, Luo Q, Li Q. On quasi-static large deflection of single lap joints under transverse loading. Thin-Walled Structures 2022;170:108572. https://doi.org/10.1016/j.tws.2021.108572.
[24] Park CH, Saouab A, Breard J, Suck Han W, Vautrin A. Integrated Optimization For Weight, Performance And Cost Of Composite Stuructures 2006;39.3: 807-812. https://doi.org/10.3182/20060517-3-FR-2903.00391.
[25] Sun G, Chen D, Zhu G, Li Q. Lightweight hybrid materials and structures for energy absorption: A state-of-the-art review and outlook. Thin-Walled Structures 2022;172:108760. https://doi.org/10.1016/j.tws.2021.108760.
[26] Tarlochan F, Samer F, Hamouda AMS, Ramesh S, Khalid K. Design of thin wall structures for energy absorption applications: Enhancement of crashworthiness due to axial and oblique impact forces. Thin-Walled Structures 2013;71:7–17. https://doi.org/10.1016/J.TWS.2013.04.003.
[27] Yilmaz Y, Çallioğlu H, Balbay A, Bölümü M.M, Fakültesi M, Üniversitesi,Investigation of quasi-static crushing and energy absorption behaviors of carbon nanotube reinforced glass fiber/epoxy and carbon fiber/epoxy composite tubular structures 2022;28:81–90. https://doi.org/10.5505/pajes.2021.68047.
[28] Molina-Moya MÁ, García-Martínez E, Miguel V, Coello J, Martínez-Martínez A. Experimental Analysis and Application of a Multivariable Regression Technique to Define the Optimal Drilling Conditions for Carbon Fiber Reinforced Polymer (CFRP) Composites. Polymers 2023;15;3710. https://doi.org/10.3390/Polym15183710.
[29] Djamaluddin F, Abdullah S, Ariffin AK, Nopiah ZM. Optimization of foam-filled double circular tubes under axial and oblique impact loading conditions 2014;87;1-11. https://doi.org/10.1016/j.tws.2014.10.015.
[30] Fang J, Gao Y, Sun G, Qiu N, Li Q. On design of multi-cell tubes under axial and oblique impact loads. Thin-Walled Structures 2015;95:115–26. https://doi.org/10.1016/J.TWS.2015.07.002.
[31] Yao R, Pang T, Zhang B, Fang J, Li Q, Sun G. On the crashworthiness of thin-walled multi-cell structures and materials: State of the art and prospects. Thin-Walled Structures 2023;189: 110734. https://doi.org/10.1016/J.TWS.2023.110734.
[32] Ataabadi PB, Karagiozova D, Alves M. Crushing and energy absorption mechanisms of carbon fiber-epoxy tubes under axial impact. Int J Impact Eng 2019;131:174–89. https://doi.org/10.1016/J.IJIMPENG.2019.03.006.
[33] Chatys R, Panich A, Jurecki RS, Kleinhofs M. Composite materials having a layer structure of "sandwich" construction as above used in car safety bumpers. 11th International Science and Technical Conference Automotive Safety, 2018:1–8. https://doi.org/10.1109/AUTOSAFE.2018.8373320.
[34] Peng Y, Hu Z, Liu Z, Che Q, Deng G. Assessment of Pedestrians' Head and Lower Limb Injuries in Tram–Pedestrian Collisions. Biomimetics 2024;9:17. https://doi.org/10.3390/BIOMIMETICS9010017.
[35] Davoodi MM, Sapuan SM, Aidy A, Abu Osman NA, Oshkour AA, Wan Abas WAB. Development process of new bumper beam for passenger car: A review. Mater Des 2012;40:304–13. https://doi.org/10.1016/J.Matdes.2012.03.060.
[36] Ganilova OA, Low JJ. Application of smart honeycomb structures for automotive passive safety. 2017;232:797–811. https://doi.org/10.1177/0954407017708916.
[37] Marques AT, Durão LM, Magalhães AG, Silva JF, Tavares JMRS. Delamination analysis of carbon fibre reinforced laminates: Evaluation of a special step drill. Compos Sci Technol 2009;69;2376–82. https://doi.org/10.1016/J.Compscitech.2009.01.025.
[38] Baba MN. Another Compression after Low-Velocity Impact Test Setup: A Case Study of Reversing the Symmetric Lay-Up for an Angle-ply CFRP Laminated Composite 2024. https://doi.org/10.20944/PreprintS202401.0168.V1.
[39] Mohamed YS, Abdelbary A. Theoretical and experimental study

on the influence of fiber orientation on the tensile properties of unidirectional carbon fiber/epoxy composite. Alexandria Engineering Journal 2023;67;693–705. https://doi.org/10.1016/J.AEJ.2022.12.058.

[40]Patel H V, Dave HK. Effect of fiber orientation on tensile strength of thin composites 2021;Vol 46;8634-8638. https://doi.org/10.1016/j.matpr.2021.03.598.

[41]Banakar P, Shivananda HK. Preparation and Characterization of The Carbon Fiber Reinforced Epoxy Resin Composites. IOSR Journal of Mechanical and Civil Engineering (IOSRJMCE) 2012;1;15–18.

[42]Keshavamurthy, Nanjundaradhya Dr, Sharma DR, Kulkarni DrRS. Investigation of Tensile Properties of Fiber Reinforced Angle Ply laminated composites 2012. https://api.semanticscholar.org/CorpusID:18468614

[43]Okon Samuel B, Saleh Yawas D, Okon Samuel B, Saleh Yawas D. A Study of the Effect of Fiber Content and Fiber Orientation on the Tensile Strength of Glass Fiber Reinforced Epoxy Composite for Pipe Production: A Taguchi and Statistical Approach 2022. https://doi.org/10.21203/RS.3.RS-1284793/V1.

[44]Raheem Z. Designation: D 7264/D 7264M-07 Standard Test Method for Flexural Properties of Polymer Matrix Composite Materials 2006;1-11.

[45]Designation: D 3039/D 3039M-00 e1 Standard Test Method for Tensile Properties of Polymer Matrix Composite Materials 2002;1-13.

[46]Raheem Z. Designation: D 7264/D 7264M-07 Standard Test Method for Flexural Properties of Polymer Matrix Composite Materials 2020;1.-15.

[47]Yee JCH, Pellegrino S. Folding of woven composite structures. Compos Part A Appl Sci Manuf 2005;36:273–8. https://doi.org/10.1016/J.Compositesa.2004.06.017.

[48]Tawfek AM, Ge Z, Yuan H, Zhang N, Zhang H, Ling Y, et al. Influence of fiber orientation on the mechanical responses of engineering cementitious composite (ECC) under various loading conditions. Journal of Building Engineering 2023;63:105518. https://doi.org/10.1016/j.jobe.2022.105518.